Broadband Dielectric Spectra of Spheroidal Hematite Particles

María L. Jiménez,[†] Francisco J. Arroyo,*[,†] Félix Carrique,[‡] and Udo Kaatze[§]

Departamento de Física Aplicada, Facultad de Ciencias, Universidad de Granada, 18071 Granada, Spain, Departamento de Física Aplicada I, Facultad de Ciencias, Universidad de Málaga, 29071 Málaga, Spain, and Drittes Physikalisches Institut, Universität Göttingen, Germany

Received: June 4, 2003; In Final Form: September 11, 2003

In this paper, we contribute new data on the dielectric dispersion of suspensions of two kinds of spheroidal hematite particles (α-Fe_2O_3). One of the samples consisted of nearly spherical particles, and the other included almost spindle-like particles. We intended to demonstrate the unique potential applications of dielectric dispersion measurements on the characterization of the electrical double layer of nonspherical particles. Thus, we show that while the electrophoretic velocity is practically the same for both systems, the dielectric spectra differ very significantly from each other. In addition to analyzing the role of axial ratios on the electrokinetic behavior, we have also focused on the effect of pH and of the frequency range in which experiments are performed. Thus, two relaxations can be identified in the suspensions: the so-called α-relaxation (typically in the kilohertz region), related to the polarization of the electrical double layer, and the Maxwell−Wagner−O'Konski relaxation (of the order of megahertz), a consequence of conductivity and permittivity mismatch between the particle and the supporting solution. We show that the dielectric increment in the α-relaxation is larger when particles have larger aspect ratio and that there is a secondary relaxation process at both low and high frequencies, a manifestation of the anisotropy of the particles. To obtain more information about this secondary relaxation, a logarithmic derivative method is used to approximate the imaginary part of the dielectric constant. The results are interpreted in the light of existing models. A qualitative agreement is found between the main features of the models and the results, although dielectric data appear to require higher ζ-potentials to be explained than electrophoresis does. We suggest that, while at low frequencies this could be a result of electrode polarization effects, data at high frequencies, less prone to be affected by such effects, confirm the existence of stagnant-layer conductivity in hematite particles.

1. Introduction

While electrokinetic techniques have been applied to solid/liquid systems of arbitrary geometry, mathematical difficulties have limited the elaboration of theoretical models for the simplest shapes, mostly flat and spherical ones.[1−7] Nevertheless, theories have been worked out that solve the problem of electrokinetic phenomena, mainly electrophoresis, for other geometries such as spheroids.[8−11] This is a very significant fact because by properly changing the axial ratio, spheroids can be used to simulate from planar to very elongated particles. It is clear that suspensions made of natural particles can be better modeled as suspensions of spheroids of certain size and axial ratio than of spheres.

In this work, we will focus on the dielectric dispersion of colloidal suspensions of spheroids. The phenomenon consists of a variation of the electric permittivity of the suspensions with the frequency of the externally applied ac field, and it has been repeatedly shown to be extremely sensitive to the characteristics of the equilibrium and nonequilibrium electrical double layer.[12,13] Probably, only difficulties sometimes involved in its experimental determination and in the elaboration of its theoretical evaluation have prevented the technique from being more widely used. Fortunately, methods have been devised to improve the experimental procedures (see below), and it is even possible to obtain useful information from the dielectric spectra without using any theoretical model[13,14] or based on approximate analytical solutions.[14,15]

Besides, it has been repeatedly suggested[6,7,16] that the greatest deal of information can be obtained if a so-called "integrated" investigation is performed. This is particularly true if the electrokinetics of the system is controlled not only by the ζ-potential but also by the conductivity in the stagnant layer, that is, the layer of immobile liquid adhered to the solid surface. In our case, dielectric dispersion data will be combined with electrophoretic mobility measurements.

The aim of this work is to show that dielectric dispersion measurements can also be used for the characterization of the solid−liquid interface in the case of nonspherical particles. To that aim, we will contribute new data on both the low-frequency (LFDD) and high-frequency (HFDD) dielectric dispersion of suspensions of spheroidal hematite (α-Fe_2O_3) particles in the 0.5 kHz to 300 MHz frequency range. Special emphasis will be placed on the role that the axial ratio and the pH play on the dielectric behavior of these dispersed systems. We hope to be able to show that dielectric dispersion can disclose aspects

* To whom correspondence should be addressed. Fax: (+34) 958 24 32 14. E-mail: fjarroyo@ugr.es.
[†] Universidad de Granada.
[‡] Universidad de Málaga.
[§] Universität Göttingen.

10.1021/jp035563m CCC: $25.00
Published on Web 10/10/2003

that are hidden in standard electrophoresis results. In particular, it will be found that the contributions of the polarization of particles oriented parallel and perpendicular to the external field can in some cases be separately observed in the frequency spectrum. The theoretical study of the dielectric constant of suspensions of spheroidal particles, performed by Grosse et al.[14,15] will guide the interpretation of our experimental results.

2. Theoretical Review

By dielectric relaxation, we mean any of the various mechanisms in virtue of which the electric permittivity of a physical system depends on the frequency of the field. All processes responsible for the finite values of the permittivity, that is, all processes explaining the polarizability of the system, need a finite time to occur. If the frequency ω of the applied field is high enough, certain mechanisms will be frozen and the permittivity will decrease.

In the case of colloidal dispersions, for the frequency range of interest, two relaxations are observed,[17] known as α-relaxation (typically occurring in the kilohertz region) and Maxwell−Wagner−O'Konski relaxation (with characteristic frequency around several megahertz).

For frequencies below the α-relaxation ($\omega \ll \omega_\alpha$), we can speak of three processes responsible for the polarizability of the suspension: molecular deformation and orientation, ion accumulation at the solid/liquid interfaces (if the ratio of the effective conductivities is different from the ratio of the permittivities), and the main mechanism related to the tangential transport of ions around the particle along its double layer and their accumulation in the low-potential side (along with their depletion at the high-potential side) of the particle (this is the configuration if the ζ-potential is negative; if it is positive, the gradient of electrolyte concentration is in the opposite direction). This process is known as concentration polarization, and it is the slowest contribution to the permittivity of the suspension. The concentration gradient needs a time $\sim\tau_\alpha = 1/\omega_\alpha$ to be established.

For frequencies above ω_α, the double layer polarization cannot take place and the slowest mechanism of polarization entails the electromigration fluxes that accumulate at the interface between the particle and the medium as the conductivity changes in this region and displacement currents, which generate bound polarization charges at the interface because of the difference in permittivities. At a certain frequency, ions transported by electromigration have not enough time to accumulate, and the permittivity relaxes again. The phenomenon is traditionally called Maxwell−Wagner relaxation. O'Konski[18] found that the presence of a conducting shell (like the double layer surrounding a nonconducting particle) can be taken into account by assigning a certain bulk conductivity to the particle's material. Because this is often the case,[7,19] the relaxation is usually called Maxwell−Wagner−O'Konski (MWO) relaxation. It has been shown that in colloids the electrokinetic features of the polarizability can be included using an asymptotic theory that employs an appropiate surface conductivity. Thus, at high ionic strengths, high potentials, and high frequencies,[19] the conduction processes on the particle surface can be considered by means of an equivalent particle surface conductivity, K^σ, that can be expressed in terms of the ζ-potential, ζ. Hence, the application of Maxwell−Wagner−O'Konski formula to colloids is usually called extended Maxwell Wagner model.[19]

Using the Maxwell procedure,[1] one can relate the dielectric constant (or relative permittivity), ϵ^*, of the suspension for each frequency ω of the field to the complex dipole coefficient, $C^*(\omega)$, of the particle:

$$\epsilon^*(\omega) = \epsilon_m^* + 3\phi\epsilon_m^* C^*(\omega) \tag{1}$$

where ϕ is the volume fraction of solids and ϵ_m^*, the complex dielectric constant of the medium, is given by ($i^2 = -1$)

$$\epsilon_m^* = \epsilon_m' - i\frac{K_m}{\omega\epsilon_0} \tag{2}$$

ϵ_0 being the permittivity of vacuum. Finally, $C^*(\omega)$ relates the induced dipole moment, $\mathbf{d}^*$, to the applied field, $\mathbf{E}$, and the particle radius, R:

$$\mathbf{d}^* = 4\pi\epsilon_0\epsilon_m' R^3 C^* \mathbf{E} \tag{3}$$

As already mentioned, there are both analytical[1,20,21] and numerical[2,22] approaches that can provide estimations of the dipole coefficient of spheres at different frequencies and hence correctly predict the α and MWO relaxations of suspensions of spherical particles. Unfortunately, there exist no similar general treatments of the dielectric dispersion in the case of spheroidal particles. For suspensions of particles with dimensions much larger than their double layer thickness, Grosse et al.[14,15] were able to solve the problem in the static case.

Introducing the dielectric increment $\delta\epsilon^*$ as the quantity accounting for the contribution of the particles to the overall dielectric constant,

$$\epsilon^*(\omega) = \epsilon_m^* + \phi\delta\epsilon^*(\omega)$$
$$\delta\epsilon^*(\omega) = \delta\epsilon'(\omega) - i\delta\epsilon''(\omega) \tag{4}$$

we calculate the zero-frequency value of its real part, $\delta\epsilon(0)$, for random particle orientation as a weighted average of the dielectric increments that would be found if the particles were parallel and perpendicular to the field:

$$\delta\epsilon(0) = \frac{\delta\epsilon_{||} + 2\delta\epsilon_\perp}{3} \tag{5}$$

where the subscript || (⊥) refers to the case when the symmetry axis is parallel (perpendicular) to the field. The result of the calculation of Grosse et al. is

$$\delta\epsilon_{||,\perp} = \frac{3\epsilon_m'\kappa^2}{16\pi ab^2}(\gamma_{||,\perp}^+ - \gamma_{||,\perp}^-)^2 I_{||,\perp} \tag{6}$$

where $2a$ is the length of the axis of revolution of the spheroid and $2b$ is the length of its perpendicular one. κ^{-1} is the Debye length or double layer thickness. The other quantities in eq 6 depend on the orientation and shape of the particles. For a prolate spheroid,

$$I_{||} = \frac{3\pi}{5h^6}\left[-a^3b^2\ln^2\frac{a+h}{a-h} + 2hb^2(a^2+b^2)\ln\frac{a+h}{a-h} + 4ah^2(a^2-2b^2)\right]$$

$$I_\perp = \frac{3\pi}{20h^6}\left[-ab^4\ln^2\frac{a+h}{a-h} + 4h(a^4+h^4)\ln\frac{a+h}{a-h} - 4ah^2(3a^2-2b^2)\right] \tag{7}$$

$$\gamma_{\parallel,\perp}^{\pm} = \frac{ab^2}{3}\frac{K_{p\parallel,\perp}^{\pm} - K_m/2}{K_m/2 + (K_{p\parallel,\perp}^{\pm} - K_m/2)A_{\parallel,\perp}} \quad (8)$$

$$h = \sqrt{a^2 - b^2} \quad (9)$$

$$K_{p\parallel}^{\pm} = \frac{3K^{\sigma\pm}a}{2bh}\left[\frac{a^2 - 2b^2}{h^2}\arctan\frac{h}{b} + \frac{b}{h}\right] \quad (10)$$

$$K_{p\perp}^{\pm} = \frac{3K^{\sigma\pm}a}{2bh}\left[\frac{a^2}{2h^2}\operatorname{arccot}\frac{b}{h} + \frac{b(a^2 - 2b^2)}{2a^2h}\right] \quad (11)$$

$$A_{\parallel} = \frac{ab^2}{h^3}\left[\operatorname{atanh}\frac{h}{a} - \frac{h}{a}\right] \quad (12)$$

$$A_{\perp} = \frac{1 - A_{\parallel}}{2} \quad (13)$$

Here $A_{\parallel,\perp}$ are the depolarization factors for prolate particles and $K_{\parallel,\perp}^{\pm}$ are the contribution of cations (+) and anions (−) to the equivalent conductivities of the particle (K_p) in the parallel (∥) and perpendicular (⊥) cases. See ref 15 for details on their calculation. Saville et al.[19] also derived the equivalent conductivity from the surface conductivity by equating the dipolar contribution to the electric field around the isolating spheroid (in which conduction takes place at the surface, K^{σ}) and around a conducting particle (the conduction takes place in the bulk, $K_{\parallel,\perp}^{\pm}$).

Although a rigorous calculation of the frequency dependence of $\delta\epsilon^*$ is not possible, Grosse et al.[14,15] assumed a Debye-like[23] relaxation function with a different characteristic frequency for each orientation. Briefly, the main results of the model are as follows: (1) The dielectric increments $\delta\epsilon_{\parallel}$ and $\delta\epsilon_{\perp}$ are higher as the surface conductivity of the particles becomes larger. $\delta\epsilon_{\parallel}$ increases with surface conductivity more strongly than $\delta\epsilon_{\perp}$. (2) The separation between the characteristic frequencies associated with the relaxations of $\delta\epsilon_{\parallel}$ and $\delta\epsilon_{\perp}$ is more evident as the axial ratio of the particles increases. (3) The contribution of parallel orientation to the total dielectric increment is larger than that of the perpendicular one.

The frequency dependence of $\delta\epsilon^*$ above the α-relaxation is described by the Maxwell−Wagner−O'Konski formula:[1]

$$\delta\epsilon_{\parallel,\perp}^* = \epsilon_m^* \frac{\epsilon_{p\parallel,\perp}^* - \epsilon_m^*}{\epsilon_m^* + A_{\parallel,\perp}(\epsilon_{p\parallel,\perp}^* - \epsilon_m^*)} \quad (14)$$

where

$$\epsilon_{p\parallel,\perp}^* = \epsilon_p - \frac{iK_{p\parallel,\perp}}{\epsilon_0\omega} \quad (15)$$

and ϵ_p is the permittivity of the particle material.

Using eq 14, we can conclude that, in the frequency range under consideration, well below the relaxation frequency of ϵ_m^* and ϵ_p, $\epsilon^*(\omega)$ is actually the result of two Debye contributions from the MWO effect, which can be associated with the relaxations that would take place in parallel and perpendicular orientations with characteristic times:

$$\tau_{\parallel,\perp} = \tau_m \frac{1 - A_{\parallel,\perp}\left(1 - \frac{\epsilon_p}{\epsilon_m}\right)}{1 - A_{\parallel,\perp}\left(1 - \frac{K_{p\parallel,\perp}}{K_m}\right)} \quad (16)$$

where

$$\tau_m = \frac{\epsilon_0\epsilon_m}{K_m} \quad (17)$$

Moreover, because the high-frequency value of the dielectric constant is related to the particle and the electrolyte permittivities through

$$\epsilon_\infty = \epsilon_m + \epsilon_{\infty\parallel} + 2\epsilon_{\infty\perp} \quad (18)$$

$$\epsilon_{\infty\parallel,\perp} = \frac{\phi}{3}\epsilon_m \frac{\epsilon_p - \epsilon_m}{\epsilon_m + A_{\parallel,\perp}(\epsilon_p - \epsilon_m)} \quad (19)$$

we can calculate both the dielectric permittivity and surface conductivity of the particles.

3. Experimental Section

3.1. Materials. The procedure described by Morales et al.[24] was used to produce two kinds of hematite particles, which we will designate as Hem1 and Hem2, that differ from one another in their average size and axial ratio. Transmission electron microscope (TEM) pictures of the two samples are displayed in Figure 1, and Table 1 includes their dimensions.

3.2. Methods. Electrophoretic mobility measurements were performed using a visual microelectrophoresis apparatus (Zeta-Meter Inc., Staunton, VA). We first used the MALVERN Zetasizer 2000, as in the majority of the recent literature. This device is based on the analysis of the autocorrelation function of the light scattered by the particles during its electrophoretic and thermal motion. However, the software of this instrument assumes that all features of the autocorrelation function are due to rectilinear motion of the particles parallel to the field, in addition to their Brownian motion. While this is true for spherical particles, spheroidal ones may also have a rotational contribution to their overall motion (and hence to the autocorrelation function) that cannot be separated by the software from the true electrophoretic displacement (see ref 17, Chapters 6 and 7). In the microelectrophoresis device, where particles are observed as individual bright points under the microscope, the operator can easily measure strictly the electrophoretic motion.

The dielectric constant at low frequencies (500 Hz to 1 MHz) was measured using a conductivity cell with variable separation between electrodes. The cell admittance was obtained as a function of frequency and electrode separation using a Hewlett-Packard HP-4284A impedance meter (Palo Alto, CA). The measurements principles can be found elsewhere.[25]

For high frequencies (300 kHz to 300 MHz), a cutoff cell working as a wave guide below its cutoff frequency was used. The cell was connected to a HP-8753A network analyzer via the HP-5044A reflection test set.[26]

Mainly in the low-frequency (kilohertz) range, electrode polarization (EP) effects constitute the most serious difficulty in performing measurements because actual relaxation phenomena can be masked by such effects, leading to a dielectric constant much higher than the true one. There are procedures that help in reducing the influence of EP on the evaluation of the permittivity. One is based on the measurement of the

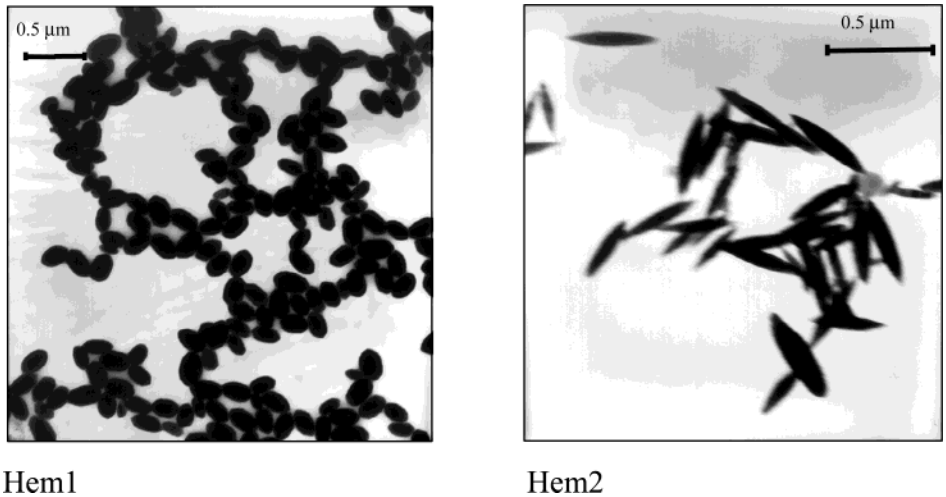

Figure 1. TEM pictures of hematite samples Hem1 and Hem2.

TABLE 1: Long and Short Axis Lengths (2*a* and 2*b*) and Axial Ratio (*a*/*b*) of Hematite Samples

	2*a* (nm)	2*b* (nm)	*a*/*b*
Hem1	469 ± 4	294 ± 3	1.595 ± 0.021
Hem2	551 ± 11	90.1 ± 2.3	6.12 ± 0.20

impedance of the cell filled with the suspension for different separations[27] and calibration of the whole system (cell and impedance meter) with a solution of known complex impedance and a conductivity similar to the suspension under study. This *quadrupole technique* (QT) appears to provide the most accurate results.[28]

We will also use a method based upon the analysis of the *logarithmic derivative* (LD) of the real part of the dielectric constant of the suspension:[29]

$$\epsilon''_{\mathrm{D}}(\omega) = -\frac{\pi}{2}\frac{\partial \epsilon'}{\partial \ln \omega} \tag{20}$$

This quantity is in fact similar to the imaginary part of $\epsilon^*(\omega)$,[29] but the interesting point is that the contribution of EP to ϵ''_{D}, which we call $\epsilon''_{\mathrm{D}}(\mathrm{EP})$ depends on the frequency and the electrode separation (L) as follows:[29]

$$\epsilon''_{\mathrm{D}}(\mathrm{EP}) \propto L^{-1}\omega^{-1.5} \tag{21}$$

whereas the contribution of EP to the true loss peak, $\epsilon''(\mathrm{EP})$ behaves as

$$\epsilon''(\mathrm{EP}) \propto \omega^{-1} \tag{22}$$

This means that, in principle, the LD method is more suitable for the separation in the frequency spectrum of the electrode polarization from the true losses because $\epsilon''_{\mathrm{D}}(\mathrm{EP})$ decreases faster with frequency than $\epsilon''(\mathrm{EP})$ does. In addition, the EP effect has been further reduced by increasing the electrode separation. A better estimation of the relaxation frequencies from experimental spectra is thus possible.

4. Results and Discussion

This section will be organized as follows: we will first present our estimations of ζ-potential based on electrophoretic mobility measurements. We will subsequently describe the dielectric dispersion data in a wide frequency band. Finally, we will discuss the surface conductivity of the particles as obtained from dielectric dispersion and from electrophoresis.

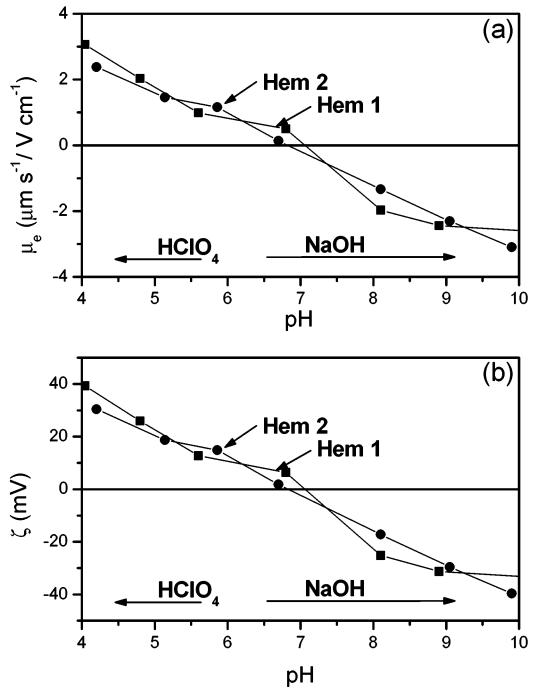

Figure 2. Electrophoretic mobility μ_e (a) and ζ potential (b) of Hem1 and Hem2 particles as a function of pH in 0.5 mM $NaClO_4$ solutions.

4.1. Electrophoresis and ζ-Potential. In Figure 2, we present the experimental values of the electrophoretic mobility, μ_e, of both hematite samples as a function of pH. The ionic strength of the medium was 0.5 mM $NaClO_4$. The mobilities of the two samples are very similar with isoelectric points between pH 7 and 8, in agreement with the visual observation that the instability of the suspensions is maximum within that pH interval. The corresponding ζ-potentials were calculated applying the Smoluchowski formula. It was used despite its simplicity, because the existing models for spheroidal particles[3,8−11] do not predict any significant deviations from Smoluchowski theory for these low-charged particles. Figure 3 demonstrates this: the ζ-potential must be at least 150 mV for the simple theory to be in serious error with either Hem1 or Hem2 samples.

4.2. Dielectric Dispersion. Figures 4−6 show the dielectric spectra (corrected for EP by means of the quadrupole method) of suspensions of Hem1 and Hem2 particles for the whole frequency range studied. In the low-frequency measurements, the volume fractions were 2% and 1%, respectively, whereas in the high-frequency measurements, ϕ was 1% and 0.8%. Let

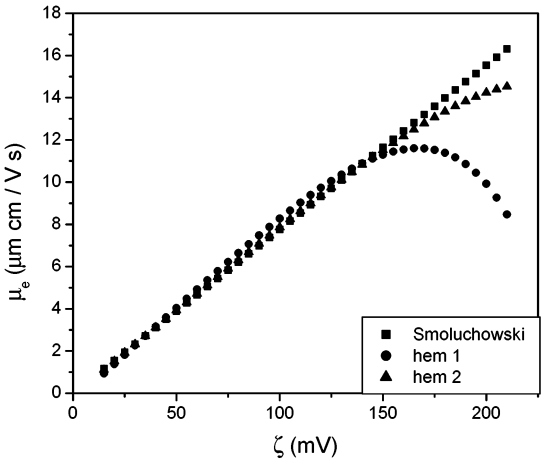

Figure 3. Predictions of both the Smoluchowski equation and the model of O'Brien and Ward[9] for the mobility of Hem1 and Hem2 particles as a function of ζ-potential in 0.5 mM $NaClO_4$ solutions.

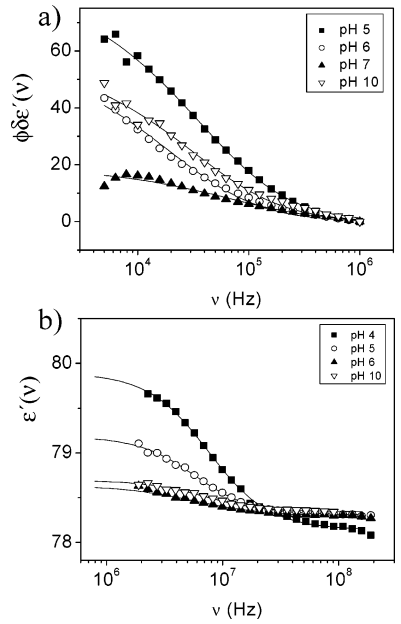

Figure 4. Dielectric spectra of Hem1 suspensions for different pH values: (a) low frequency, $\phi = 2\%$; (b) high frequency, $\phi = 1\%$. Ionic strength = 0.5 mM NaCl. Lines are the best fit to eq 23.

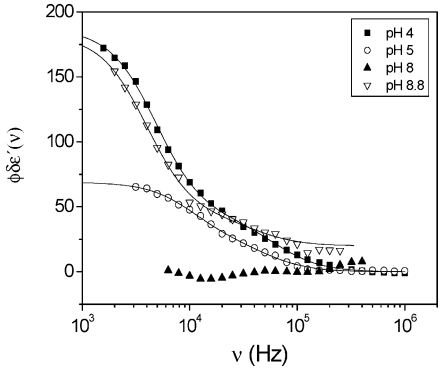

Figure 5. Dielectric spectra of Hem2 suspensions and $\phi = 1\%$ for different pH values at low frequency. Ionic strength = 0.5 mM NaCl. Lines are the best fit to eq 24.

us point out that dielectric dispersion measurements in hematite are difficult because of the low surface charge of the particles at natural pH values and the relatively large density of this material, which prevented us from using more concentrated

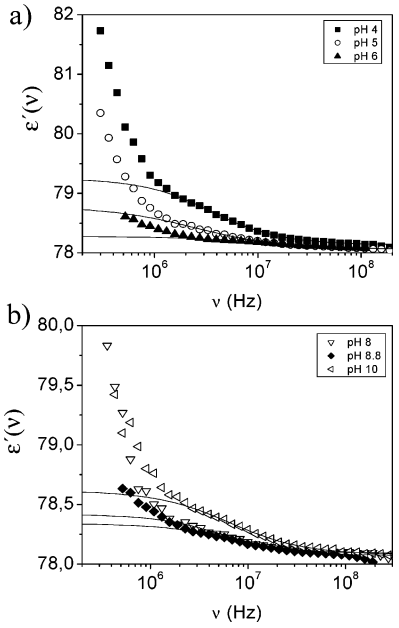

Figure 6. Dielectric spectra of Hem2 suspensions and $\phi = 0.8\%$ for different pH values at high frequency: (a) pH 4, 5, and 6; (b) pH 8, 8.8, and 10.

dispersions. The electrolyte concentration was 0.5 mM NaCl in all systems. Note that the anion in this case differs from that used for electrophoresis measurements (ClO_4^-), but the diffusion coefficient of ClO_4^- anions, $D(ClO_4^-) = 1.8 \times 10^{-9}$ m^2 s^{-1}, is similar to that of Cl^-, $D(Cl^-) = 2.0 \times 10^{-9}$ m^2 s^{-1}. Figure 4 demonstrates that the least elongated particles, Hem1, only show one relaxation in each frequency range; the characteristic frequencies corresponding to both orientations are not sufficiently separated to enable a clear resolution of the relaxation terms, a result that qualitatively agrees with the theory of Grosse et al., which predicts a smaller separation between $\tau_{||}$ and $\tau_{\perp}$ when the axial ratio of the particles is smaller.

For these reasons, the data in Figure 4 were fitted, for both the low- and high-frequency range, to a Cole−Cole relaxation function:[24]

$$\epsilon^*(\omega) = \mathrm{Re}\left\{\epsilon_\infty + \frac{\phi\delta\epsilon(0)}{1 + (i\omega\tau)^{1-\beta}}\right\} \qquad (23)$$

In this function, τ is a measure of the characteristic relaxation time, and β gives information about the width of the relaxation. It must be noted that this function describes a symmetrical relaxation (the imaginary component of $\epsilon^*(\omega)$ is a symmetrical bell-shaped curve). Nevertheless, whatever the shape of the particles, asymmetrical curves are found in the dielectric spectra of their suspensions (e.g., see refs 1−3, 17, and 21). A relaxation function like the Dukhin−Shilov's one (demonstrated for spherical particles)[1] might be more suitable, but one peculiarity of the spheroidal particles is that their relaxation is wider than that in the spherical case. As a consequence, the Dukhin−Shilov function does not reproduce the shape of the experimental curves. An alternative could be the Havriliak−Negami expression,[23] which has two parameters that take into account the asymmetry and the width of the dispersion. We will use it later in the determination of relaxation frequencies, but now our aim is not to find the actual function but the dielectric increment. On the other hand, the data fit well to the simpler Cole−Cole function, which allows us to take into account the width of the relaxation curve without necessarily fitting a large number of parameters, although we have to neglect the asymmetry of the

TABLE 2: Parameters of the Best Fit of the Dielectric Spectrum of Hem1 Suspensions (Figure 4) to a Cole−Cole Function (Eq 23)[a]

pH	$\delta\epsilon_\alpha(0)$	τ_α (μs)	β_α	$\delta\epsilon_{MWO}(0)$	τ_{MWO} (ns)	β_{MWO}	ϵ_∞
4				177 ± 6	21.2 ± 0.9	0.077 ± 0.020	78.134 ± 0.014
5	4390 ± 70	4.9 ± 0.4	0.33 ± 0.03	88 ± 3	27.6 ± 1.2	0.055 ± 0.021	78.306 ± 0.007
6	3200 ± 100	14.0 ± 0.9	0.33 ± 0.04	36 ± 8	28 ± 9	0.18 ± 0.6	78.234 ± 0.006
7	1130 ± 30	2.6 ± 0.4	0.23 ± 0.09				
10	3090 ± 100	10.1 ± 0.9	0.42 ± 0.07	35 ± 2	23.5 ± 1.5	0.06 ± 0.04	78.343 ± 0.007

[a] Subscripts α and MWO refer to the α- and Maxwell−Wagner−O'Konski relaxations, respectively.

TABLE 3: Parameters of the Best Fit of the Dielectric Spectrum of Hem2 Suspensions (Figures 5 and 6) to a Two-Debye-Term Model (Eq 24) for Low Frequency and to a Cole−Cole Function (Eq 23) for High Frequency

Low Frequency

pH	$\delta\epsilon_1(0)$	τ_1 (μs)	$\delta\epsilon_2(0)$	τ_2 (μs)
4	14550 ± 140	32.6 ± 0.7	4150 ± 120	2.55 ± 0.13
5	4500 ± 300	14.8 ± 1.2	2400 ± 300	3.1 ± 0.4
8.8	14100 ± 700	40 ± 4	2100 ± 500	3.8 ± 1.3

High Frequency

pH	$\delta\epsilon_{MWO}(0)$	ϵ_∞	τ_{MWO} (ns)	β_{MWO}
4	141 ± 4	78.129 ± 0.005	44.7 ± 2.0	0.181 ± 0.013
5	91.4 ± 1.1	78.053 ± 0.007	64 ± 14	0.278 ± 0.04
6	27.6 ± 1.9	78.058 ± 0.005	13.1 ± 0.9	0.29 ± 0.04
8	41 ± 4	78.090 ± 0.005	31 ± 4	0.174 ± 0.04
8.8	33.8 ± 1.8	78.070 ± 0.003	23.6 ± 1.5	0.19 ± 0.03
10	69 ± 3	78.072 ± 0.004	24.3 ± 1.6	0.24 ± 0.02

curve. Table 2 shows the best-fit parameters. Note that both dielectric increments, $\delta\epsilon_\alpha(0)$ and $\delta\epsilon_{MWO}(0)$, mainly the former, are very sensitive to the pH of the systems and are in fact minimum at the vicinity of the isoelectric point. Let us mention that the lack of stability of the suspensions for such pH prevented us from measuring the high-frequency permittivity because the rapidly sedimenting particles did not yield reproducible results.

It is worth mentioning here that while in electrophoresis Hem1 and Hem2 particles behave similarly (Figure 2); the situation is completely different in the dielectric spectra (compare Figures 4 and 5). Not only is the dielectric increment at low frequency larger in Hem2 samples, but most importantly, the shapes of the relaxation curves differ significantly from one another.

Two relaxations are observed in the more elongated Hem2 systems, one at about 30 kHz and the other at around 300 kHz. Hence, we decided to fit these results with two Debye relaxations, each with its corresponding relaxation time, τ_1 and τ_2 respectively, so that we may associate the relaxations of the parallel and perpendicular orientation:

$$\epsilon^*(\omega) = \epsilon_\infty + \phi\frac{\delta\epsilon_1(0)}{1 + i\omega\tau_1} + \phi\frac{\delta\epsilon_2(0)}{1 + i\omega\tau_2} \qquad (24)$$

The parameters of this function that best fit our data in Figure 5 are displayed in Table 3 (except for pH 8, at which no relaxation is observed but rather an unexpected increase of ϵ' with frequency, which must be due to experimental errors due to aggregation during the measurement of these low-charged particles; the signal-to-noise ratio close to the isoelectric point of the particles is necessarily low). Note that $\delta\epsilon_1(0)$ is larger than $\delta\epsilon_2(0)$ and $\tau_1 > \tau_2$; hence, we can relate $\delta\epsilon_1(0)$ and τ_1 to the α relaxation corresponding to parallel orientation. We can justify this assignment as follows. Recall that the rather high values often found for the dielectric constant of colloidal suspensions at low frequencies are a manifestation of displacement currents, out of phase with respect to the external field and induced by the electrolyte concentration gradient associated

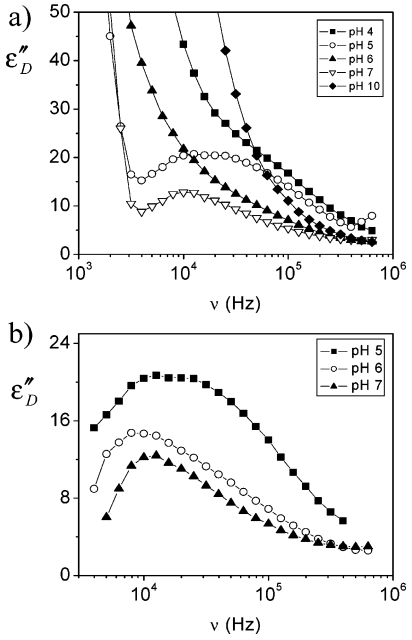

Figure 7. Low-frequency ϵ''_D spectra (eq 20) of Hem1 suspensions at different pHs: (a) with EP effects; (b) after eliminating EP effects where possible in panel a. Ionic strength = 0.5 mM NaCl. Volume fraction = 2%.

with the phenomenon of concentration polarization. The distance to the particle surface at which the concentration changes occur is of the order of the particle size. The larger that distance is, the longer the characteristic time τ becomes and the larger the displacement current becomes.[1] This explains that parallel orientation of the prolate spheroid brings about longer relaxation times and larger dielectric increments.

At high frequencies, Figures 4b and 6 demonstrate that, whatever the axial ratio (low in Figure 4b, corresponding to Hem1; high in Figure 6, for Hem2), the relaxation frequencies for different orientations are not well separated and hence we can only observe a relaxation somewhat broadened with respect to a Debye term.

A Cole−Cole function was also fitted to the data of Hem2 suspensions, and the values of the fitting parameters are also included in Table 3. The most interesting feature of these parameters is again the fact that the amplitude of the MWO relaxation, represented by $\delta\epsilon_{MWO}$, reaches a minimum in the pH = 7−9 range, where the isoelectric point is known to be (Figure 2).

As already mentioned, in principle, the LD method turned out to be more suitable for the detection of $\tau_{||}$ and $\tau_\perp$ as separated times in dielectric spectra. Hence we repeated the data treatment of the dielectric dispersion of Hem1 and Hem2 but now using the logarithmic derivative. Figure 7 corresponds to Hem1 at low frequencies. Note that at very low frequency EP effects fully mask the relaxation, and the method could in fact be used only at pH 5, 6, and 7. Fitting the low-frequency data to a power law of the form $\epsilon''_D(EP) \propto \omega^{-m}$,[29] we could subtract the electrode

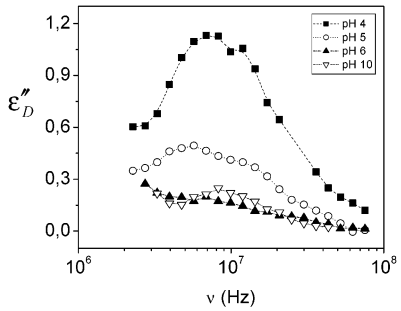

Figure 8. High-frequency ϵ''_D spectra (eq 20) of Hem1 suspensions at different pHs. Ionic strength = 0.5 mM NaCl. Volume fraction = 1%.

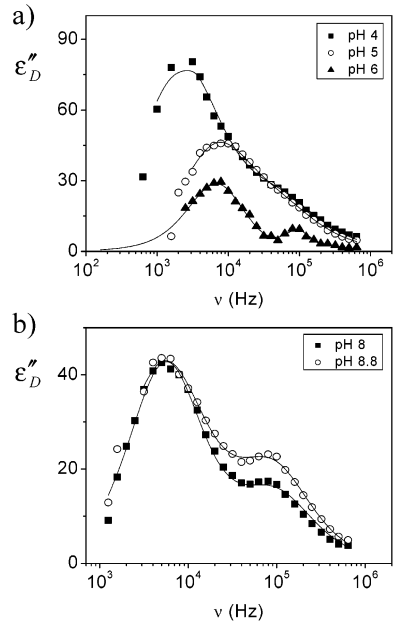

Figure 9. Low-frequency spectra of ϵ''_D (eq 20) for Hem2 suspensions at different pHs: (a) pH 4, 5, and 6; (b) pH 8 and 8.8. Ionic strength = 0.5 mM NaCl. Volume fraction = 1%. Lines are the best fit to eq 25.

polarization from the full spectra, and the results of Figure 7b were obtained. It is interesting to notice that the width of the peaks suggest indeed the presence of two superimposed relaxations. In Figure 8, it is shown that the two relaxations can be better distinguished in the high-frequency spectrum, particularly at pH 4 and 5, when the amplitude of the dielectric dispersion is highest.

The larger axial ratio of Hem2 particles makes them most suitable for the application of the method. Figures 9 (low frequency) and 10 (high frequency) are a clear proof of this. As predicted by the model of Grosse et al.,[14,15] the separation of the two α-relaxation processes is more evident when the surface conductivity is lower (pH is closer to the isoelectric point). To make our discussion more quantitative, we have fitted $\epsilon''_D(\omega)$ data to the logarithmic derivative of the sum of two Havriliak−Negami functions,[23] one for each orientation:

$$\epsilon''_D(\mathrm{HN}) = -\frac{\pi}{2}\frac{\partial \epsilon'_{||}(\mathrm{HN})}{\partial \ln \omega} - 2\frac{\pi}{2}\frac{\partial \epsilon'_{\perp}(\mathrm{HN})}{\partial \ln \omega} \qquad (25)$$

with

$$\epsilon'_{||,\perp}(\mathrm{HN}) = \mathrm{Re}\left\{\epsilon_\infty + \phi\frac{\delta\epsilon_{||,\perp}(0)}{[1+(i\omega\tau_{||,\perp})^{a_{||,\perp}}]^{b_{||,\perp}}}\right\} \qquad (26)$$

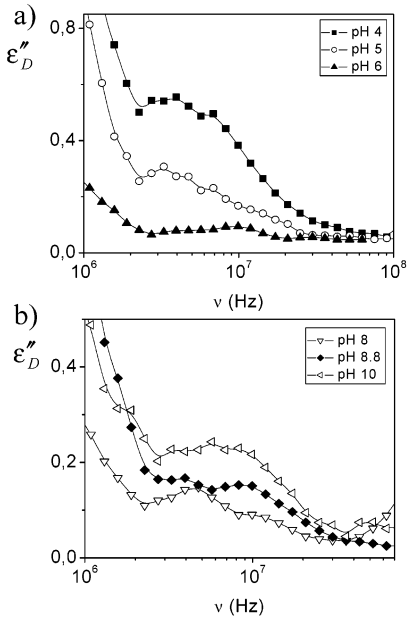

Figure 10. High-frequency spectra of ϵ''_D (eq 20) for Hem2 suspensions: (a) pH 4, 5, and 6; (b) pH 8, 8.8, and 10. Ionic strength = 0.5 mM NaCl. Volume fraction = 0.8%. Lines are a guide to the eye.

TABLE 4: Parameters of the Best Fit to Eq 25 for the Spectra of Hem2 (Figure 9) Obtained with the LD Method

	Low Frequency			
pH	$\delta\epsilon_{\|\|}(0)$	$\tau_{\|\|}$ (μs)	$\delta\epsilon_{\perp}(0)$	$\tau_{\perp}$ (μs)
4	9090 ± 100	70.2 ± 1.7	970 ± 40	2.88 ± 0.22
5	4450 ± 200	23.1 ± 0.5	780 ± 90	2.88 ± 0.22
6	2350 ± 100	20 ± 4	150 ± 40	1.7 ± 0.3
8	3590 ± 90	28.7 ± 0.3	610 ± 50	1.63 ± 0.06
8.8	4150 ± 200	29.6 ± 0.7	770 ± 60	1.71 ± 0.08

Let us point out that in the case of the imaginary component of ϵ^* (and hence when the logarithmic derivative is calculated) consideration of the symmetry is very important if we are interested in finding the characteristic frequency of the relaxation. For this reason, we decided to use the more general function of Havriliak and Negami (of which the Cole−Cole function is a particular case).

In Table 4, we present the best-fit values of $\delta\epsilon_{||,\perp}(0)$ and $\tau_{||,\perp}$. Concerning the fitting parameters not shown, let us mention that the values of a (both $a_{||}$ and $a_\perp$) were between 0.75 and 0.9 and those of b (both $b_{||}$ and $b_\perp$) were between 0.9 and 1.2. The results suggest that our analysis is consistent; both $\delta\epsilon$ and τ are larger for parallel orientation, when ions must move along the long axis of the spheroid. Further, whatever the orientation considered, the amplitudes and relaxation times are lowest for the central pH range, close to the isoelectric point.

4.3. Surface Conductivity. According to the model by Grosse et al.,[14,15] the low-frequency dielectric constant of suspensions of spheroids depends (in addition to the volume fraction of particles) on the particle dimensions and on their surface conductivity, K^σ. Note that in Hem1 and Hem2 systems, $\kappa b \geq 15$ and 5, respectively, and the model of Grosse et al. is valid only when both κa and κb are $\gg 1$, so it would be little suitable for the smallest particles. However, it is the only approach available for the calculation of the dielectric constant of suspensions of spheroidal particles, and we have used it with the two systems, although our calculations must be considered as estimations when dealing with Hem2. From LFDD data in Figures 4a and 5, K^σ can be estimated using this theory. Further on, one can assume that the surface conductivity is completely

TABLE 5: Surface Conductivity K^σ and ζ-Potential of Hem1 Particles[a]

pH	K^σ (10^{-9} S)	ζ_α (mV)	ζ_u (mV)
5	0.35	68.5	26
6	0.25	58.6	13
7	0.091	34.6	6
10	0.17	−60.9	−32

[a] K^σ was calculated from $\delta\epsilon(0)$ values using the model of Grosse et al.[15,16] ζ_α is the ζ-potential corresponding to K^σ according to Bikerman's equation (eq 27). ζ_u is the ζ-potential from electrophoresis data (Figure 2).

TABLE 6: Surface Conductivity of Hem2 Spheroids[a]

pH	$K^\sigma_{\|\|}$ (10^{-9} S)	$K^\sigma_\perp$ (10^{-9} S)	$\zeta_{\alpha\|\|}$ (mV)	$\zeta_{\alpha\perp}$ (mV)	ζ_u (mV)
4	6.75	0.27	195	60.5	30.5
5	2.52	0.20	148	52.5	18.7
6	1.33	0.037	119	20.3	14.9
8	1.86	0.056	−147	−39.4	−10.2
8.8	2.17	0.076	−154	−44.5	−26.4

[a] $K^\sigma_{||}$ ($K^\sigma_\perp$) data were deduced from $\delta\epsilon_{||}$ ($\delta\epsilon_\perp$) in Table 4. $\zeta_{\alpha||}$ ($\zeta_{\alpha\perp}$) were calculated from the corresponding surface conductivities by means of Bikerman's equation (eq 27). ζ_u is the ζ-potential from electrophoresis measurements (Figure 2).

due to the ionic transport in the diffuse part of the ionic atmosphere, and hence. it is controlled by the ζ-potential, ζ. At this hypothesis, the classical calculation of K^σ is due to Bikerman,[7] and its final expression is

$$K^\sigma = \frac{2e^2z^2n}{k_BT\kappa}\left[D^+(e^{-ze\zeta/(2k_BT)} - 1)\left(1 + \frac{3m^+}{z^2}\right) + D^-(e^{ze\zeta/(2k_BT)} - 1)\left(1 + \frac{3m^-}{z^2}\right)\right] \quad (27)$$

where n is the number concentration of the z-valent symmetrical electrolyte, k_B is the Boltzmann constant, and m^+ (m^-) is the ionic mobility of cations (anions):

$$m^\pm = \frac{2\epsilon_0\epsilon_m}{3\eta}\left(\frac{k_BT}{e}\right)^2\frac{1}{D^\pm} \quad (28)$$

η being the viscosity of the fluid. From this, the ζ-potential can be calculated. For sample Hem1, Table 5 includes K^σ and ζ_α (ζ deduced as just described), together with the ζ-potential obtained from electrophoresis, ζ_u (Figure 2). Note that dielectric spectra do not inform us directly about the sign of ζ, so we used electrophoresis data to identify that sign. Table 5 shows that, while K^σ values are of a reasonable magnitude, the ζ-potentials calculated from them are too high when compared to ζ_u. We believe that the reason for such overestimation cannot be electrode polarization, which always tends to increase the apparent $\delta\epsilon$. In fact, this is quite a general finding, not only with LFDD data but also with other kinds of measurements, such as dc conductivity.[4,30−34] An alternative explanation assumes that ions in the stagnant layer can contribute to surface conductivity. This "stagnant-layer conductivity" has been demonstrated to contribute positively to $\delta\epsilon$.[17,20,35,36] Furthermore, experimental data and numerical simulations[37] show that the diffusion coefficients of ions in the stagnant layer may be equal to those in the bulk (particularly in the case of monovalent ions).

Table 6 contains the data for Hem2 suspensions. In this case, K^σ can be calculated independently from $\delta\epsilon_{||}(0)$ and $\delta\epsilon_\perp(0)$ (see Table 4); the most significant feature of Table 6 is that $|\zeta_{\alpha||}| > |\zeta_{\alpha\perp}|$. Because the characteristic frequency for $\delta\epsilon_{||}$ is lower than that of $\delta\epsilon_\perp$, it is likely that the former is more influenced by EP. Nevertheless, even the absolute value of $\zeta_\perp$ is larger than that of ζ_u; it is likely that $\delta\epsilon_\perp(0)$ (and hence $\zeta_\perp$) is not affected by electrode polarization. No other explanation than stagnant layer conductivity seems plausible in this case.

TABLE 7: Surface Conductivity and ζ-Potential of Hem1 and Hem2 Particles Estimated from High-Frequency Dielectric Measurements

pH	K^σ_{Hem1} (10^{-9} S)	K^σ_{Hem2} (10^{-9} S)	$\zeta_{MWO,Hem1}$ (mV)	$\zeta_{MWO,Hem2}$ (mV)
4	7.89	2.14	203	140
5	3.22	1.03	159	108
6	1.64	0.58	128	86
8		0.78		−110
8.8		0.58		−99
10	1.61	0.92	−140	−117

This is in fact confirmed by high-frequency data. Using eqs 18 19, we could obtain the permittivity of hematite particles from the high-frequency values of the permittivity of the suspensions. The results obtained ($\epsilon_p = 35$ and 27 for Hem1 and Hem2 particles) are rather close to the literature value[38] ($\epsilon_p = 25$). With this information and the low-frequency limit of eq 9, we could calculate K^σ and from it the ζ-potential of the particles. The results are shown in Table 7. Note that the ζ-potentials explaining the observed relaxation amplitudes are even higher than those in the α-relaxation case (compare with Tables 5 and 6).

This is a consequence of the fact that the total surface conductivities obtained from the megahertz range are higher than those of the kilohertz range data, probably in part because of the limited precision attained when the high contribution of the left part of the plots (see Figure 6) is subtracted. Despite these divergences, both the high- and low-frequency estimations of the surface conductivity behave qualitatively in similar ways: K^σ increases as we depart from the isoelectric point, and it tends to be larger for Hem1 particles as compared to Hem2, although for the latter particles $K^\sigma_{||}$ does not follow that trend because of the already mentioned electrode effect contaminating $K^\sigma_{||}$ data.

5. Conclusions

The dielectric spectra of suspensions of nonspherical particles exhibit new aspects that are absent in spherical particle systems. We have shown the strong effect of the axial ratio on the spectra, a significant feature of dielectric dispersion data, considering that its effect on the electrophoretic mobility is very low. The dielectric constant at low frequencies exhibits two relaxations, in agreement with the theoretical predictions of Grosse et al. for spheroidal particles. The separation between both relaxations is possible for large aspect ratios, although the secondary relaxation process is partially masked by the primary one at high surface conductivity.

We have investigated the possibility of calculating the ζ-potential from every relaxation process. Although there is a qualitative agreement between these results and those found with electrophoresis, dielectric data systematically lead to higher ζ-potentials. The principal reason seems to be the presence of a nonzero stagnant-layer contribution to surface conductivity, which is not taken into account in the classical Bikerman's equation. The results at high frequency, where the electrode polarization effects are significantly reduced, confirm the existence of a high surface conduction in the stagnant layer.

Acknowledgment. Financial support for this work by MCyT, Spain (Projects MAT 2001-3803 and BFM 2000-1099), and FEDER funds is gratefully acknowledged.

References and Notes

(1) Dukhin, S. S.; Shilov, V. N. *Dielectric Phenomena and the Double Layer in Disperse Systems and Polyelectrolytes*; Wiley: New York, 1974.
(2) DeLacey, E. H. B.; White, L. R. *J. Chem. Soc., Faraday Trans. 2* **1981**, *77*, 2007.
(3) Arroyo, F. J.; Carrique, F.; Delgado, A. V. *J. Colloid Interface Sci.* **1999**, *210*, 194.
(4) Minor, M.; van Leeuwen, H. P.; Lyklema, J. *J. Colloid Interface Sci.* **1998**, *206*, 397.
(5) Dukhin, S. S.; Derjaguin, B. V. In *Surface and Colloid Science, vol. 7: Electrokinetic Phenomena*; Matijeviæ, E., Ed.; Wiley: New York, 1974.
(6) Hunter, R. J. *Foundations of Colloid Science*; Oxford University Press: Oxford, U.K., 2001.
(7) Lyklema, J. *Fundamentals of Interface and Colloid Science, vol. II: Solid−Liquid Interfaces*; Academic Press: New York, 1995.
(8) Fair, M. C.; Anderson, J. L. *J. Colloid Interface Sci.* **1989**, *127*, 388.
(9) O'Brien, R. W.; Ward, D. N. *J. Colloid Interface Sci.* **1988**, *121*, 402.
(10) Kim, J. Y.; Yoon, B. J. *J. Colloid Interface Sci.* **2002**, *251*, 318.
(11) Grosse, C. *J. Phys. Chem.* **1989**, *93*, 5865.
(12) Arroyo, F. J.; Carrique, F.; Jiménez-Olivares, M. L.; Delgado, A. V. *J. Colloid Interface Sci.* **2000**, *229*, 118.
(13) Arroyo, F. J.; Delgado, A. V.; Carrique, F.; Jiménez, M. L.; Bellini, T.; Mantegazza, F. *J. Chem Phys.* **2002**, *116*, 10973.
(14) Grosse, C.; Shilov, V. N. *J. Colloid Interface Sci.* **1997**, *193*, 178.
(15) Grosse, C.; Pedrosa, S.; Shilov, V. N. *J. Colloid Interface Sci.* **1999**, *220*, 31.
(16) Dukhin, S. S. *Adv. Colloid Interface Sci.* **1995**, *61*, 17.
(17) Delgado, A. *Interfacial Electrokinetics and Electrophoresis*; Surfactant Science Series; Marcel Dekker: New York, 2002.
(18) O'Konski, C. T. *J. Phys. Chem.* **1960**, *64*, 605.
(19) Saville, D. A.; Bellini, T.; Degiorgio, V.; Mantegazza, F. *J. Chem. Phys.* **2000**, *113*, 6974.
(20) Shilov, V. N.; Delgado, A. V.; González-Caballero, F.; Grosse, C. *Colloids Surf., A* **2001**, *192*, 253.
(21) Grosse, C.; Tirado, M. C.; Pieper, W.; Pottel, R. *J. Colloid Interface Sci.* **1998**, *205*, 26.
(22) Mangelsdorf, C. S.; White, L. R. *J. Chem. Soc., Faraday Trans.* **1998**, *94*, 2441.
(23) Böttcher, C. J. F.; Bordewijk, P. *Theory of Electric Polarization*; Elsevier Scientific: Amsterdam, 1978; Vol. II.
(24) Morales, M. P.; González-Carreño, T.; Serna, C. J. *J. Mater. Res.* **1992**, *7*, 2538.
(25) Carrique, F. Ph.D. Thesis, University of Granada, Granada, Spain, 1993.
(26) Göttmann, O.; Kaatze, U.; Petong, P. *Meas. Sci. Technol.* **1996**, *7*, 525.
(27) Schwan, H. P. Determination of biological impedances. In *Physical Techniques in Biological Research*; Nastuk, W. L., Ed.; Academic Press: New York, 1963; Vol. 6, pp 323−406.
(28) Grosse, C.; Tirado, M. *Mater. Res. Soc. Symp. Proc.* **1996**, *430*, 287.
(29) Jiménez, M. L.; Arroyo, F. J.; van Turnhout, J.; Delgado, A. V. *J. Colloid Interface Sci.* **2002**, *249*, 327.
(30) Zukoski, C. F.; Saville, D. A. *J. Colloid Interface Sci.* **1986**, *114*, 45.
(31) Midmore, B. R.; Hunter, R. J. *J. Colloid Interface Sci.* **1988**, *122*, 521.
(32) Midmore, B. R.; Diggins, D.; Hunter, R. J. *J. Colloid Interface Sci.* **1989**, *129*, 153.
(33) Löbbus, M.; van Leeuwen, H. P.; Lyklema, J. *Colloids Surf., A* **2000**, *161*, 103.
(34) Lyklema, J.; Minor, M. *Colloids Surf., A* **1998**, *140*, 33.
(35) Lyklema, J.; van Leeuwen, H. P.; Minor, M. *Adv. Colloid Interface Sci.* **1999**, *83*, 33.
(36) Dukhin, S. S.; Zimmermann, R.; Werner, C. *Colloids Surf., A* **2001**, *195*, 103.
(37) Arroyo, F. J.; Carrique, F.; Bellini, T.; Delgado, A. V. *J. Colloid Interface Sci.* **1999**, *210*, 194.
(38) Sverjensky, D. A. *Geochim. Cosmochim. Acta* **2001**, *65*, 3643.